Solid State Communications 249 (2017) 44–47

Contents lists available at ScienceDirect

Solid State Communications

journal homepage: www.elsevier.com/locate/ssc

Communication

Integer quantum Hall effect in a triangular-lattice: Disorder effect and scaling behavior of the insulator-plateau transition

H.L. Yu[a,b,*], C. Jiang[a], Z.Y. Zhai[a,b]

[a] School of Physics and Electronic Electrical Engineering, Huaiyin Normal University, Huaian 223300, China
[b] National Laboratory of Solid State Microstructures and Department of Physics, Nanjing University, Nanjing 210093, China

ARTICLE INFO

Keywords:
Integer quantum Hall effect
Chern number
Quantum phase transition

ABSTRACT

We investigate numerically the integer quantum Hall effect in a three-band triangular-lattice model. The three bands own the Chern number C=2,−1,−1, respectively. The lowest topological flat band carrying Chern number C=2, which leads to the Hall plateau $\sigma_H = 2(e^2/h)$. This Hall plateau is sensitive to the disorder scattering and is rapidly destroyed by the weak disorder. Further increasing the strength of disorder, the gap of density of states always disappears before the vanishing of the corresponding Hall plateau. The scaling behavior of quantum phase transition between an insulator and a quantum Hall plateau is studied. We find that the insulator-plateau transition becomes sharper with increasing the size of system. Due to the different of edge states, the critical energy E_{c1} gradually shifts to the center of Hall plateau while E_{c2} is unaffected with increasing the disorder strength.

1. Introduction

The integer quantum Hall effect (IQHE) is discovered experimentally by Kliziting in 1980 [1], in which the transverse Hall conductivity of a two-dimensional (2D) system of electrons is found to have plateaus in the presence of a strong perpendicular magnetic field [1,2]. Immediately after this discovery, scientists from various disciplines were launched into a frenzy of activity to understand the underling physics and also to explore its technological importance in designing different electronic devices. The first theoretical work on this effect was put forward by Laughlin [3] based on a gauge-invariance argument, and further theoretical elaboration was made possible through the picture of edge states by Halperin [4]. However, it is also natural to explain the realization of the IQHE by explicit calculations based upon the linear-response Kubo formula for periodic systems [5]. The electron energy spectrum is split into discrete Landau levels. If the Fermi level lies exactly between two Landau levels, the Hall conductance can be labeled by topological Chern number in units of e^2/h and be accurately quantized to an integer.

The Anderson localization theory [6,7] predicts that non-interacting electrons in 2D disordered system in the absence of a magnetic field are generally localized with time-reversal and spin rotational symmetries. However, the time-reversal symmetry is broken by external magnetic field, and a series of Landau bands appear due to disorder. The interplay between magnetic field and disorder is an essential issue for the phenomenon of IQHE. There are many theoretical studies focusing on the existence of a plateau-insulator transition [8–11] in 2D electronic system with an external magnetic field. The energy spectrum in a uniform magnetic field for a square lattice was investigated by Hofstadter [12] and since then the electronic properties of 2D periodic lattice structures immersed in a uniform magnetic field have drawn a lot of interests and been hot topics among theoreticians [11,13–22]. Sheng et al. [11,14–16] studied the IQHE at strong disorder and weak magnetic field in the tight-binding lattice model, where the systematic float-up and merging picture for extended level was found. The Scaling behavior of the quantum phase transition between an insulator and a quantized Hall plateau state or between two adjacent plateau states has been examined by realizing landau levels. A nonzero integer Chern number distinguishes an extended state from a localized state (Chern number is zero) in the system. So they suggested that topological characterization in terms of Chern integers provide a simple physical explanation and gives a qualitative difference between the lattice and continuum models.

Though most of the theoretical studies based on the lattice structure with a uniform magnetic field has been performed, a very few theoretical works [23–25] are available where the multi-band lattice model has been used. However, the effects of the disorder strength on the transition between an insulator and a quantum Hall plateau and the scaling behavior of the quantum phase transition have not been studied in the multi-band lattice model. We wish to address these

* Corresponding author at: School of Physics and Electronic Electrical Engineering, Huaiyin Normal University, Huaian 223300, China.
E-mail address: hlyu_phys@126.com (H.L. Yu).

http://dx.doi.org/10.1016/j.ssc.2016.10.015
Received 14 September 2016; Accepted 31 October 2016
Available online 04 November 2016
0038-1098/

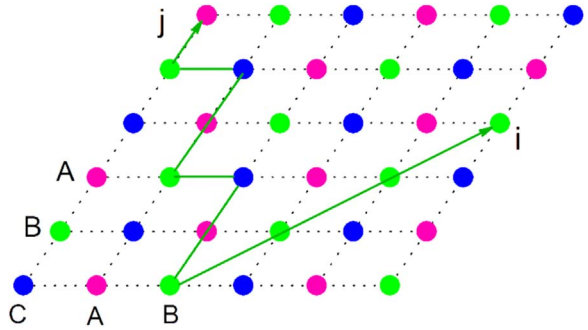

Fig. 1. Schematic diagram of a 2D triangular-lattice with three single-particle bands labeled by pink (A), green (B) and blue (C)circle dots, respectively. (For interpretation of the references to color in this figure legend, the reader is referred to the web version of this article.)

issues in the present work.

In this paper, we will study in detail numerically the Hall conductance and density of states (DOS) using the exact diagonalization method and Kubo formula. The model and theoretical method are described in the next section while the numerical results and related discussions are given in Section 3. In Section 4 our results are briefly summarized.

2. The model and theoretical method

We consider a 2D triangular-lattice as shown in Fig. 1. It is characterized by three single-particle bands (A, B and C) per unit cell. Creation (a_{ij}^+, b_{ij}^+, c_{ij}^+) and annihilation (a_{ij}, b_{ij}, c_{ij}) operators are introduced, where i(j) stands the site index along the direction of arrow. The tight-binding (TB) Hamiltonian is employed to describe our system and it reads as

$$\begin{aligned} H = \sum_{i,j} & w_{ij}(a_{ij}^+ a_{ij} + b_{ij}^+ b_{ij} + c_{ij}^+ c_{ij}) + [t(b_{i,j+2}^+ + b_{i,j-1}^+ + b_{i+1,j-1}^+ - c_{i,j+1}^+ \\ & - e^{2i\phi}c_{i+1,j+1}^+ - e^{-2i\phi}c_{i+1,j-2}^+) + t'e^{i\phi}(a_{i+1,j}^+ + a_{i-1,j+3}^+ + a_{i,j-3}^+) \\ & + t'e^{-i\phi}(a_{i-1,j}^+ + a_{i+1,j-3}^+ + a_{i,j+3}^+)]a_{ij} + [t(a_{i,j+1}^+ + a_{i-1,j+1}^+ + a_{i,j-2}^+ \\ & + c_{i+1,j-1}^+ + e^{-2i\phi}c_{i,j+2}^+ + e^{2i\phi}c_{i,j-1}^+) + t'e^{i\phi}(b_{i-1,j}^+ + b_{i,j+3}^+ + b_{i+1,j-3}^+) \\ & + t'e^{-i\phi}(b_{i+1,j}^+ + b_{i,j-3}^+ + b_{i-1,j+3}^+)]b_{ij} + [t(-a_{i,j-1}^+ - e^{2i\phi}a_{i-1,j+2}^+ \\ & - e^{-2i\phi}a_{i-1,j-1}^+ + b_{i-1,j+1}^+ + e^{2i\phi}b_{i,j-2}^+ + e^{-2i\phi}b_{i,j+1}^+) \\ & - t'(c_{i+1,j}^+ + c_{i-1,j}^+ + c_{i+1,j-3}^+ + c_{i,j+3}^+ + c_{i,j-3}^+ + c_{i-1,j+3}^+)]c_{ij}, \end{aligned} \tag{1}$$

where the nearest-neighbor and next-nearest-neighbor hoppings are considered in Eq. (1), $w_{ij}$is a disorder potential energy uniformly distributed between $(-W/2, W/2)$ on site (note that the disorder strength W here is as big as that defined in Ref. [11]), t (t') is the hopping integral between the nearest (next-nearest) neighboring sites, ϕ is the azimuthal angle for the vector connecting hopping.

Assuming that the lattice is composed of N_1 and N_2 number of sites along the i- and j-directions, respectively, where N_2 is a multiple of 3, and the total number of lattice sites is $N = N_1 \times N_2$. With the choice of $W = 0$ and employing the Fourier transform $c(k_x, k_y) = \frac{1}{\sqrt{N_1 N_2}}\sum_{i_x j_y} c_{ij} e^{i(k_x i_x + k_y j_y)}$, the k-representation of Hamiltonian is described by a 3×3 matrix as following:

$$H = \sum_{\vec{k}} (a_{\vec{k}}^+ \quad b_{\vec{k}}^+ \quad c_{\vec{k}}^+) \begin{pmatrix} H_{11} & H_{12} & H_{13} \\ H_{21} & H_{22} & H_{23} \\ H_{31} & H_{32} & H_{31} \end{pmatrix} \begin{pmatrix} a_{\vec{k}} \\ b_{\vec{k}} \\ c_{\vec{k}} \end{pmatrix}. \tag{2}$$

Here,

$$\begin{cases} H_{11} = t'[2\cos(k_x + \phi) + 2\cos(k_x - 3k_y - \phi) + 2\cos(3k_y - \phi)] \\ H_{22} = t'[2\cos(k_x - \phi) + 2\cos(k_x - 3k_y + \phi) + 2\cos(3k_y + \phi)] \\ H_{33} = t'[2\cos k_x + 2\cos 3k_y + 2\cos(k_x - 3k_y)] \\ H_{12} = H_{21}^* = t(e^{ik_y} + e^{i(-k_x + k_y)} + e^{-2ik_y}) \\ H_{13} = H_{31}^* = -t(e^{i(-k_x + 2k_y + 2\phi)} + e^{-i(k_x + k_y + 2\phi)} + e^{-ik_y}) \\ H_{23} = H_{32}^* = t(e^{i(k_y - 2\phi)} + e^{i(-k_x + k_y)} + e^{2i(-k_y + \phi)}) \end{cases}.$$

we adopt the parameters $t = 1$, $t' = 1/4$, $\phi = 2\pi/6$, and use the periodic boundary conditions. The energy spectrum of the triangular-lattice is shown in Fig. 2(a) and (b). It is found that the topological flat band states are well created and the two gaps are verified between sub-bands.

After the numerical diagonalization of the Hamiltonian (Eq. (1)), the Hall conductance can be calculated by using the Kubo formula [5,13]:

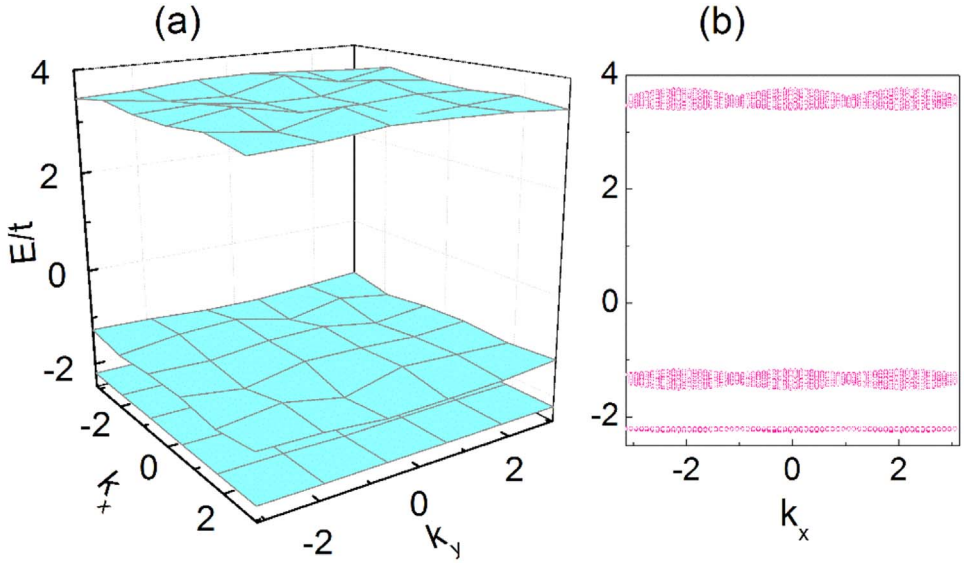

Fig. 2. The energy spectrum of the 2D triangular-lattice model. (b) is the cut plane of (a). The lowest topological flat band is obtained.

$$\sigma_H(\varepsilon) = \frac{ie^2\hbar}{A_0} \sum_{\varepsilon_m<E<\varepsilon_n} \frac{\langle m|v_x|n\rangle\langle n|v_y|m\rangle - \langle m|v_y|n\rangle\langle n|v_x|m\rangle}{(\varepsilon_m - \varepsilon_n)^2}. \quad (3)$$

Here, A_0 is the area of the system, E is the Fermi energy, ε_m and ε_n are the corresponding eigenvalues of the eigenstates $|m\rangle$ and $|n\rangle$. The velocity operator is defined as $v_\tau = (1/i\hbar)[\hat{\tau}, \hat{H}]$, where $\hat{\tau}$ is the position operator of electrons along x- or y-direction. And Hall conductance can be rewritten as

$$\sigma_H(\varepsilon) = e^2/h \sum_{\varepsilon_m < E} C_m. \quad (4)$$

Here, C_m is the Chern number of the m th sub-band being always an integer.

Throughout our numerical calculations, we set $T = 0K$, the lattice constant $a = 1$, the hopping integral $t = 1$,$t' = 1/4$, the azimuthal angle $\phi = 2\pi/6$, where $c = e = h = 1$ is chosen and energies are measured in units of t.

3. Numerical results and discussions

First, the case of clean limit ($W = 0$) is considered with the size of $N = 24 \times 24$. The Hall conductance together with the corresponding DOS versus the Fermi energy E are shown in Fig. 3. Two well-defined Hall plateaus $\sigma_H = \nu e^2/h (\nu = 2, 1)$ are clearly shown by blue circles, corresponding to three Landau-level subbands (see the pink line) centered at the jumps of the Hall conductance. The energy gaps between sub-bands clearly shown by the energy spectrum in Fig. 2 is also well revealed by DOS=0 in Fig. 3, which gives the widths of the Hall plateaus. It is well-known that a nonzero Chern number characterizes an extended state in the IQHE. And the boundary-condition-averaged Hall conductance is a summation of all those Chern numbers carried by states below Fermi surface, which is described by Eq. (4). When the Fermi surface is located in the left peak, the Chern number is found to be exactly 2, which leads to the Hall plateau with $\sigma_H = 2(e^2/h)$. The right two peaks all own Chen number $C = -1$.

Since all the states in a 2D electron system in the absence of a magnetic field are localized due to disorder, which is predicted by Anderson localization theory, the situation is somewhat interesting when impurities are introduced into the system. We introduce a random onsite potential with strength $|w_{ij}| \le W/2$ into our system. The Fermi energy dependence of Hall conductance for different disorder strength (W=1, 2, 3, 7, 9 and 11) is shown in Fig. 4, and the corresponding DOS is plotted in Fig. 5. In presence of disorder, such as W=1 (weak disorder), labeled by blue circles in Fig. 4, the two Hall plateaus are well-defined, but their widths narrow down a little

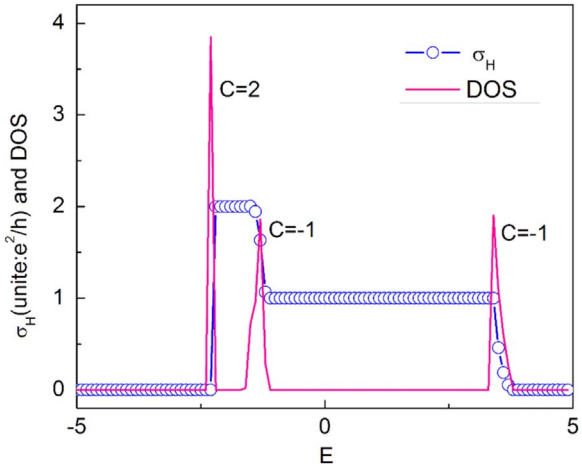

Fig. 3. The Hall conductance σ_H (blue circle-line) and DOS (pink line) versus the Fermi energy E for the perfect (W=0) 2D triangular-lattice with the size of N=24×24. (For interpretation of the references to color in this figure legend, the reader is referred to the web version of this article.)

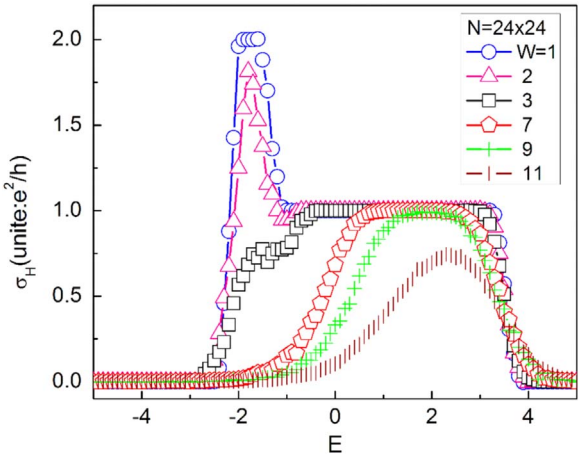

Fig. 4. The Hall conductance σ_H as a function of Fermi energy E is plotted for different disorder strength W in sequence, {1,2,3,7,9,11}, at the lattice size of 24×24. The Hall plateau with Chern number C=2 is destroyed rapidly by the weak disorder. All the data points do not intersect during the left transition from $\sigma_H = 0$ to $\sigma_H = e^2/h$ but they intersect at one point during the right transition from $\sigma_H = e^2/h$ to $\sigma_H = 0$. (For interpretation of the references to color in this figure, the reader is referred to the web version of this article.)

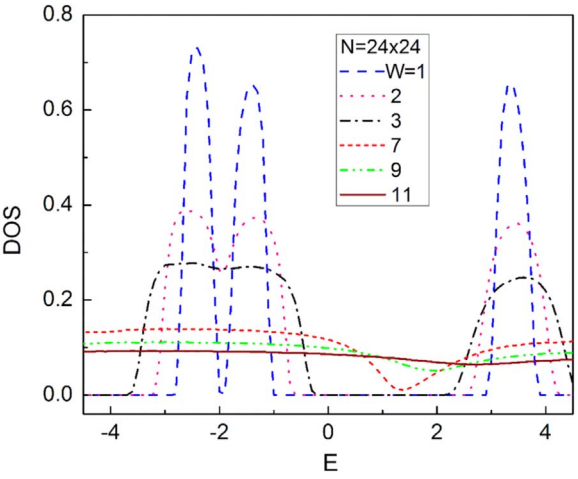

Fig. 5. Energy dependence of the density of states (DOS) corresponding Hall conductance shown in Fig. 4. When the disorder strength W is weak, the left two peaks rapidly began to merge while the right peak remains well separated. (For interpretation of the references to color in this figure, the reader is referred to the web version of this article.)

compared with the case of W=0 shown in Fig. 3. At the same time, the picks of the corresponding DOS located at the centers of Landau-level bands decrease and become wider with narrowing the widths of gaps shown by blue line in Fig. 5. And it is found that the left peak with Chern number C=2 goes down more rapidly than the other peaks with Chern number C=−1. With the disorder strength further enhanced, the width of the Hall plateau and the gap of DOS become narrow gradually, meanwhile, the values of DOS located at centers of Landau-level bands decrease and begin to merge due to disorder. Such as, when W increases to 2 and 3, the left two peaks start to merge. Because these peaks carry total Chern numbers of +2 and −1, respectively, a mixing and annihilation of these Chern numbers results in a disappearance of the left Hall plateau $\sigma_H = 2(e_2/h)$. By contrast, the right peak remains well separated (see the black line in Fig. 5), which persuades the well-defined Hall plateau $\sigma_H = e^2/h$ (see the black squares in Fig. 4). Further increasing the strength of disorder, the rest gap of DOS vanishes at W=7 shown by red line in Fig. 5, but the corresponding Hall plateau still exists with narrower width (see red pentagons in Fig. 4), and finally this Hall plateau disappears at W=11(see the wine symbols). At the

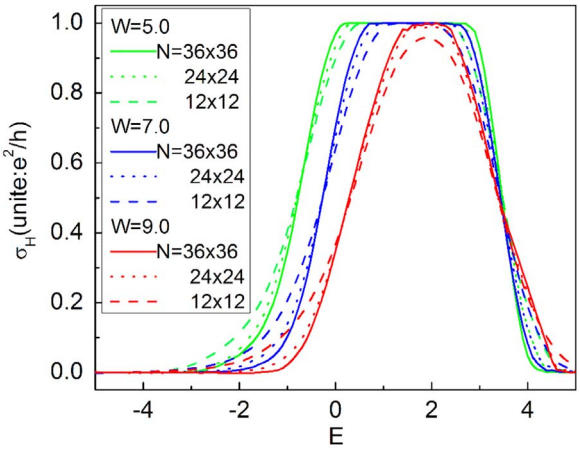

Fig. 6. The evolution of Hall conductance σ_H with the Fermi energy E for different system sizes from N=12×12 to 36×36, at the disorder strength of W=5.0(green lines), W=7.0(blue lines), W=9.0(red lines). For the fixed W (such as W=7.0, see blue lines), all data points cross at the critical energy E_{c1} (the left) and E_{c2} (the right). (For interpretation of the references to color in this figure legend, the reader is referred to the web version of this article.)

disorder W=11, the extended states are changed qualitatively by strong disorder, which leads to the completely merged DOS shown by wine solid line in Fig. 5. We also find that the jump of Hall conductance from zero to plateau $\sigma_H = e^2/h$ shifts to the center of Hall plateau with increasing the disorder strength and all the data lines for the different disorder strength do not intersect during the jump process. On the other hand all the data lines intersect at one point during the jump of Hall conductance from plateau $\sigma_H = e^2/h$ to zero.

Finally we study the scaling behavior of the quantum phase transition. The effects of the system size on the Hall conductance for different disorder strength (green lines for W=5, blue lines for W=7, red lines for W=9) are shown in Fig. 6. For the fixed value of disorder strength (such as W=5), the Hall conductance σ_H continuously increases from zero to the quantized value e^2/h and then decreases from Hall plateau to zero, with data for different system sizes crossing at each other. With increasing the size of system, The crossovers of insulator-plateau transition become sharper (dashed line for N=12×12, dotted line for N=24×24 and solid line for N=36×36), which consists with a quantum phase transition at the thermodynamic limit where a step jump of Hall conductance should occur [26]. We define that E_{c1} is a critical energy at the left crossing point from insulator to plateau and E_{c2} is the right one from plateau to insulator. It is found that E_{c2} is unaffected by the disorder strength, and all the data lines intersect at one point for different disorder strength. But the critical energy E_{c1} decreases gradually and shifts to the center of the Hall plateau with increasing the disorder strength. The critical energy E_{c1} and E_{c2} are located at the jumps of Hall conductance. The different edge states lead the different effects of disorder scattering on E_{c1} and E_{c2}.

4. Summary

We have studied the IQHE in a 2D triangular lattice with three bands. The tight-binding Hamiltonian is applied to describe the model and Kubo formula is performed to numerically calculate the Hall conductance. The flat bands and the finite gaps between these bands are verified, which results in Chern numbers in sequence, {2,−1,−1}. It was found that the Hall plateau with Chern number C=2 was destroyed rapidly by the weak disorder. The other Hall plateau with Chern number C=1 became narrow down gradually and finally disappeared with increasing the disorder. On the other hand, the peaks of DOS located at the centers of Landau-level sub-bands began to merge, which leads to the narrowing down in the gap of DOS, and finally the disappearance of the gap was always earlier than the vanishing of the corresponding Hall plateau. Scaling behavior of the insulator-plateau transition was also studied in our present work, which indicated that this transition became sharper with increasing the size of system and all the data lines intersect at the critical energy E_{c1} or E_{c2} during the transitions. Due to the different of edge states, E_{c1} gradually shifts to the center of plateau but E_{c2} is fixed at one point with increasing the disorder strength.

Acknowledgments

We are especially grateful to Professor D. N. Sheng for discussions. This work was supported by the Natural Science Foundation of Jiangsu Province (Grant No. BK20140450), Huaian Science and Technology (Industry) Project (Grant No. HAG2014043).

References

[1] K.V. Klitzing, G. Dorda, M. Pepper, Phys. Rev. Lett. 45 (1980) 494.
[2] D.C. Tsui, H.L. Stormer, A.C. Gossard, Phys. Rev. Lett. 48 (1982) 1559.
[3] R.B. Laughlin, Phys. Rev. B 23 (1981) 5632.
[4] B.I. Halperin, Phys. Rev. B 25 (1982) 2185.
[5] D.J. Thouless, M. Kohmoto, M.P. Nightingate, M. den Nijs, Phys. Rev. Lett. 49 (1982) 405.
[6] E. Abrahams, P.W. Anderson, D.C. Liccardello, T.V. Ramakrishnan, Phys. Rev. Lett. 42 (1979) 673.
[7] P.A. Lee, T.V. Ramakrishnan, Rev. Mod. Phys. 7 (1985) 287.
[8] F. Wegner, Nucl. Phys. B 316 (1989) 663.
[9] S. Hikami, A.I. Larkin, Y. Nagaoka, Prog. Theor. Phys. 63 (1980) 707.
[10] T. Ando, Phys. Rev. B 40 (1989) 5325.
[11] D.N. Sheng, Z.Y. Weng, Phys. Rev. Lett. 78 (1997) 318.
[12] D.R. Hofstadter, Phys. Rev. B 14 (1976) 2239.
[13] P. Dutta, S.K. Maiti, S.N. Karmakar, J. Appl. Phys. 112 (2012) 044306.
[14] D.N. Sheng, Z.Y. Weng, Phys. Rev. Lett. 80 (1998) 580.
[15] D.N. Sheng, Z.Y. Weng, X.G. Wen, Phys. Rev. B 64 (2001) 165317.
[16] D.N. Sheng, L. Sheng, Z.Y. Weng, Phys. Rev. B 73 (2006) 233406.
[17] Y.F. Wang, C.D. Gong, Phys. Rev. Lett. 98 (2007) 096802.
[18] J. Li, Y.F. Wang, C.D. Gong, J. Phys.: Condens. Matter 23 (2011) 156002.
[19] J. Priest, S.P. Lim, D.N. Sheng, Phys. Rev. B 89 (2014) 165422.
[20] S.K. Maiti, M. Dey, S.N. Karmakar, Phys. Lett. A 376 (2012) 1366.
[21] G.G. Naumis, Phys. Lett. A 380 (2016) 1772.
[22] R. Keil, C. Poli, M. Heinrich, J. Arkinstall, G. Weihs, Phys. Rev. Lett. 116 (2016) 213901.
[23] Y. Zhang, A. Vishwanath, Phys. Rev. B 87 (2013) 161113(R).
[24] M. Nita, B. Ostahie, A. Aldea, Phys. Rev. B 87 (2013) 125248.
[25] Y.F. Wang, H. Yao, C.D. Gong, D.N. Sheng, Phys. Rev. B 86 (2012) 201101(R).
[26] Y. Huo, R.N. Bhatt, Phys. Rev. Lett. 68 (1992) 1375.